RSC Advances

PAPER

Cite this: *RSC Adv.*, 2016, **6**, 77709

Inorganic layered double hydroxides as a 4-hexyl resorcinol delivery system for topical applications

Damodar Mosangi,[abc] Sreejarani Kesavan Pillai,[a] Lumbidzani Moyo[a] and Suprakas Sinha Ray*[ab]

Received 28th July 2016
Accepted 9th August 2016

DOI: 10.1039/c6ra19195a

www.rsc.org/advances

In this study, the hydrophobic even skin tone active, 4-hexylresorcinol (HR), was intercalated into a zinc aluminium layered double hydroxide (ZnAl-LDH) by a co-precipitation method and used as a controlled release ingredient in skin care formulation. The resulting nanohybrid (LDH–HR) was characterized using different techniques: XRD, FTIR, TEM, SEM, and TGA. The intercalation reaction between HR and LDH was confirmed using XRD, and FTIR. Some extent of aggregation was observed for the LDH–HR nanoparticles from TEM and SEM results. The thermal behaviour of HR drastically improved after intercalation into the LDH host. Strong electrostatic interactions between the HR and ZnAl-LDH galleries in the nanohybrid and the sustained release of HR from the LDH–HR in phosphate buffered saline (PBS) were observed. We also investigated the de-pigmenting efficiency of the LDH–HR nanohybrid containing formulations in randomized controlled experiments, which showed impressive results after 14 days of topical applications. The LDH–HR nanohybrid significantly minimized the melanogenesis in primary human melanocytes, resulting in overall improvements in even skin tone. Based on the above results, we believe that the LDH–HR nanohybrid has high potential for use as an alternative active ingredient in topical applications for uneven skin tone.

1 Introduction

Nowadays, the development of nanocarrier-mediated drug delivery systems is a significantly important research area in pharmaceuticals, which has been used to decrease the negative side effects, increase the therapeutic activity, minimize the frequency of administration, and maintain the concentration of drugs for some time.[1] The use of such advanced technologies in cosmetic active ingredient release has garnered interest as well. In general, inorganic nanoparticles are good nanocarriers for various applications due to their unique properties such as high drug loading efficiency, biocompatibility, and distinct stability. Therefore, numerous inorganic nanocarriers including calcium phosphate,[2] silica oxide,[3] magnetite,[4] gold,[5] platinum,[6] carbon,[7] and layered double hydroxide (LDHs)[8] have been studied for the delivery of pharmaceutically active drugs. LDH is a new class of synthetic 2D lamellar materials with positively charged layers and charge balancing anions situated in the interlayer region. The general formula of LDH is $[M_{1-x}^{2+}M_x^{3+}(OH)_2]_x + (A_x/n^{n-})\cdot mH_2O$, where M^{2+} and M^{3+} are divalent and trivalent metal ions, respectively, A^{n-} is the anion, and m is the quantity of water (H_2O) present in the inter-lamellar region. LDHs are potential candidates for carrying pharmaceutical active substances owing to their anion-exchange capacity, stable structure, biocompatibility, controllable particle size, and high drug loading efficiency.[1,9] Hence, most of the active ingredients (organic anions) such as amino acids,[10–12] vitamins,[12–14] pesticides,[15,16] medicine,[4,17–19] and DNA[20,21] are encapsulated into LDH layers in order to form molecular reservoirs[22,23] in slow and controlled release systems (CRS).[24–28] However, oral and injection delivery is generally used for the administration of drug-LDH nanocomposites.[29,30]

Uneven skin tone is a common, typically inoffensive disorder in which patches of skin become darker in colour than the surrounding skin due to excessive production of melanin. Therefore, uneven skin tone solutions are of communal and cosmetic interest to people, since most of the skin problems are found on highly visible parts of the body, such as the face, forearms, and hands. Physical or topical therapy is used to overcome these problems.[31–33] Physical therapy (laser, pulsed light, cryotherapy, and chemical peels) produces rapid and substantial improvement, but clinically expert personnel are necessary for the administrations of such therapy. It can also be expensive and may lead to certain detrimental side effects, such as swelling, redness, post-inflammations, and even scarring of the skin. In contrast, topical treatment employs one or more inhibitors of pigmentation as an even toning technique. The most commonly used inhibitors to control pigmentation by

[a]*DST-CSIR National Centre for Nanostructured Materials, Council for Scientific and Industrial Research, Pretoria 0001, South Africa. E-mail: rsuprakas@csir.co.za*

[b]*Department of Applied Chemistry, University of Johannesburg, Droonfontein 2028, Johannesburg, South Africa*

[c]*Innovation Building, AMKA Products Pvt. Ltd., 14 Ellman Street, Suderland Ridge, Centurion 0157, Pretoria, South Africa*

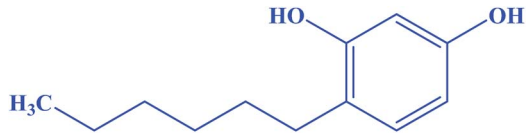

Fig. 1 Chemical structure of 4-hexyl resorcinol.

affecting the transcription and activity of pigmentary enzymes are peroxidase, tyrosinase, tyrosinase-related protein-1 (Tyrp-1), tyrosinase-related protein-2 (Tyrp-2), methimazole, ellagic acid and hydroquinone.[34–36] Among the different skin lightening agents, hydroquinone has been the most frequently used in numerous even tone formulations for more than 5 decades.[37–39] However, the use of hydroquinone has several drawbacks: it is unstable in alkaline medium, it is a skin irritant that can also induce hypersensitivity reactions, and above all, it is allegedly a carcinogen.[40–42] Thus, the development of a safe and effective active ingredient for even skin tone is of paramount importance in cosmetic applications.

4-Hexylresorcinol (HR) has been used in topical disinfectants, throat lozenges, and food products for a long time owing to its anti-oxidant and antimicrobial activities and GRAS (generally regarded as safe) status.[43–47] HR, with 4-substituted resorcinol molecules (see Fig. 1), and compounds with similar chemical structure are well known as potent inhibitors of tyrosinase activity *in vitro*.[48,49] However, more recently, the potential melanotoxic effect of the HR molecule has been reported, and the de-pigmenting efficiency of HR in numerous *in vitro* prototypes in a randomized controlled clinical study has been done by Won *et al.*[50] in which they observed a significant improvement in depigmentation/even skin tone over a period of 3 months. In order to decrease this time period, a new active ingredient delivery system that can facilitate as faster skin-absorption and controlled release is required. Our previous studies (results not published) revealed the potential of ZnAl-LDH in the controlled release of and in stabilizing cosmetic active ingredients. However, to the best of our knowledge, an even skin tone active ingredient delivery system based on LDHs has not been reported so far. Therefore, we thought it worthwhile to develop a new class of HR-intercalated ZnAl-LDH nanohybrids and to perform control release studies *in vitro* and *in vivo* for topical applications.

2 Experimental sections

Chemicals and reagents

Aluminium nitrate hexa hydrate ($Al(NO_3)_3 \cdot 6H_2O$) (99%), zinc nitrate ($Zn(NO_3)_2$) (98%) and sodium hydroxide (98%) were obtained from Sigma-Aldrich (South Africa); HR (>99%) from Sython (USA); propylene glycol from Dow chemicals (USA); EDTA, xanthan gum, triethanolamine (99%), allantoin, vitamin E, aluminium starch octenylsuccinate, and ethylhexylmethoxycinnamate from IMCD (South Africa); glycerol monostearate, PEG-100 stearate, and PPG-15 stearyl ether from Croda (UK); potassium cetylphosphate from DSM (Switzerland); ceteary alcohol from Ecogreen (Malaysia); stearylcaprylate and heptonate from Symrise (Germany); dimethicone from Dow corning (USA); mineral oil from Akulu (South Africa); iodopropynylbutylcarbamate, and methylisothiazolinone from Thor Personal Care (UK).

In situ intercalation of HR into ZnAl-LDH using the co-precipitation method

100 mL mixed solution of 2 M $Zn(NO_3)_2$ and 1 M $Al(NO_3)_3 \cdot 6H_2O$ was added to 80 mL 1 M solution of HR in acetone. 1 M NaOH was added drop-wise under constant stirring, while adjusting the pH to 9–10. The stirring was continued until solutions were completely mixed, after which the precipitate was filtered and washed with a large volume of de-ionized water until all the NO_3^- ions were removed. The obtained solid was allowed to dry overnight at room temperature before drying for 24 h in a convention oven at 60 °C. The dried sample was then ground into a powder and sieved to 80 μm particle size for further analysis. ZnAl– LDH was prepared as a reference material using a similar procedure without the use of HR. The schematic model of the developed nanohybrid is shown in Fig. 2.

Development of a topical formulation containing a LDH–HR nanohybrid

Topical skin formulations were prepared using the ingredients shown in Table 1. Both the oil phase containing a LDH–HR nanohybrid and the water phase were heated to 70 °C. After both the phases reached the desired temperature, the oil phase was combined into the water phase and mixed for 5 min using a Silverson high shear mixer at 3000 rpm. The neutralizer was then added, and the whole mixture was mixed for another 5 min using the same homogenizer at 3000 rpm. The mixture was then cooled to 40 °C and a preservative was added to obtain the LDH–HR based emulsion. The same procedure was followed for the formulation with only neat HR with concentration corresponding HR loading in LDH (0.25%). The pH of the final formulation was adjusted to 5.6. The stability of the formulations was checked at 25 °C, 37 °C and 50 °C for 6 weeks and no phase separation was found.

Nanohybrid characterization

X-ray diffraction (XRD) studies were conducted using an X'Pert PRO X-ray diffractometer (PANalytical, Netherlands) operating with Cu K-α radiation (wavelength of 0.15406 nm) at 45 kV and 40 mA. The exposure time and scan speed for the XRD measurements were 19.7 min and 0.036987° s^{-1}, respectively. HR intercalation into the LDHs was followed using Fourier

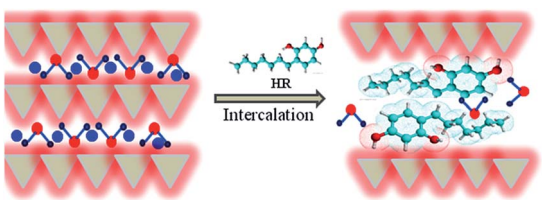

Fig. 2 Schematic representation of HR intercalated into the LDH host.

Table 1 Constituents of the formulations used in the current study

Entry	Ingredients	Percentage (%)
1	Deionized water	QS
2	Stearic acid	8
3	Ethylhexylmethoxycinnamate	8
4	PEG-100 stearate	6
5	Glycerol mono stearate	6
6	Aluminium starch octenylsuccinate	4
7	Mineral oil	2
8	Propylene glycol	6
9	Stearylcaprylate	4
10	Stearylheptonate	4
11	PPG-15 stearyl ether	3
12	LDH–HR	1
13	Potassium cetyl phosphate	2
14	Cetearyl alcohol	6
15	Xanthan gum	2
16	TEA	1
17	Disodium EDTA	0.2
18	Dimethicone	2
19	Perfume	0.5
20	Preservative	0.02

transform infra-red spectroscopy (Perkin-Elmer Spectrum 100 spectrometer, USA) with the MIRacle ATR attachment and a Zn/Se crystal. A small amount of sample was pressed onto the Zn/Se crystal, showing spectra over the range of 550 to 4000 cm^{-1}. Morphological changes on the surfaces of the neat LDHs and HR-intercalated LDHs before and after the intercalation were studied using scanning electron microscopy (JEOL, JSM 7500F, Japan) under a 3 kV acceleration voltage. The intercalated HR particle dispersion in the LDHs was directly visualized using high-resolution transmission electron microscopy (JEOL JEM 2100 HRTEM) operated at 200 kV acceleration voltage. The particle size distribution was obtained by Image J V.1.36B software. For TEM analysis, the powder samples were sonicated in ethanol for 1 minute and dropped on a carbon coated Cu-grid and dried. Particle size, polydispersity as well as zeta-potential were measured at 25 °C on a Litesizer™ 500 (Anton Paar Instruments, Austria). The particle size analyses were done in disposable plastic cuvettes after dispersing the material is silicon oil whereas omega cuvettes and deionized water medium were used for zeta potential measurements. Thermogravimetric analysis (TGA) of neat LDHs, HR, and LDH–HR were performed using TGA (TA instruments, model Q500, USA). The temperature was ramped at 10 °C min^{-1} in air, from 25 °C to 900 °C. The drug loading capacity of LDH was determined from the residue weight percentage analysis.

In vitro release studies of HR from LDH–HR nanohybrid

To measure the amount of HR released from the LDH–HR nanohybrids, *in vitro* release tests were performed as follows: 0.1 g of the LDH–HR nanohybrid was added to 100 mL of phosphate buffer saline (PBS) solution in a closed beaker at room temperature. At regular time intervals after the addition of the nanohybrid, 5 mL of the solution was withdrawn (the volume of PBS was maintained by adding fresh PBS) and filtered using a polyvinylidene fluoride micro syringe filter. The amount of HR in the nanohybrid samples was measured by UV-Vis spectroscopy (Perkin Elmer Lamda 750, USA) at $\lambda_{max} = 296$ nm based on UV-Vis absorption spectrum of neat HR. The data were collected in triplicate.

In vivo studies of LDH–HR nanohybrid-based topical formulation

The study of skin care formulation efficacy was carried out at Amka Products Pty Ltd (Skin care laboratory, South Africa). Safety and ethical clearance for the study was obtained from both the University of Johannesburg and Amka R&D skin care (South Africa). Four healthy South African female panelists, aged 20–50 years, were recruited and classified as possessing hyper-pigmented or pale axillae, on the basis of an instrumental measurement (Mexameter MX-18, Courage + Khazaka Electronic GmbH, Cologne, Germany).

A patch test was initially conducted to measure possible skin reactivity in each volunteer. The 'neat HR' formulation patch was applied on the right side, while the 'nanohybrid' formulation patch was applied on the left side of each volunteer's forearm skin (0.16 g on 2 cm × 2 cm area). After 24 h, each volunteer's forearm skin was checked at 25 ± 3 °C under 60 ± 5% RH for any undesirable reactions (skin hypersensitivity such as eventual itching, irritation, rash, erythema, desquamation, oedema, other sensation of discomfort). The volunteers were instructed to apply a cream at least twice per day and to not use any other type of topical creams for a period of at least two weeks. Individual skin and potential skin reactivity were checked every day for 3 weeks except on weekends. The assessment was based on the determination of the effects of the creams on the production of skin melanin, erythema, and moisture using non-invasive instruments (Mexameter). Measurements were done in duplicates and the average values are reported.

3 Results and discussion

Nanohybrid characterization

In order to assess the formation of the nanohybrid prepared using co-precipitation method and intercalation of active ingredient, we studied the XRD pattern of the LDH–HR nanohybrid together with that of the neat ZnAl-LDH, and the XRD patterns are illustrated in Fig. 3. The neat ZnAl-LDH shows well-defined (003) peaks at lower 2θ values and clear (110) reflection at higher 2θ, indicating the formation of LDHs.[51] In the present work, the interlayer *d*-spacing of LDH–NO_3^- was 0.85 nm, which is very close to the value of 0.86 nm reported by Zhang *et al.*[52] According to Olanrewaju *et al.*,[53] *d*-spacing of 0.86 nm corresponds to NO_3^- form of the LDHs due to the difference in number and orientation of anions in the interlayer in comparison to the value of 0.76 nm observed for CO_3^{2-} form. The slight variation in *d*-spacing is probably because a small amount of the interlayer spaces are engaged by carbonate ions (CO_3^{2-}) provided by the ionization of carbon dioxide (O=C=O) dissolved in the distilled water used.[54] However, the relative

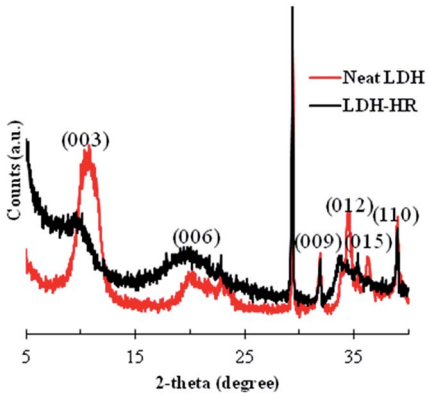

Fig. 3 The XRD patterns of ZnAl LDH and LDH–HR nanohybrid.

intensity of the XRD pattern of unmodified LDH is indicative of its highly crystalline nature.[55] This may be attributed to the fact that $Zn(OH)_2$ can fit together well enough to form a more stable crystalline phase.[56] However, in the case of HR-intercalated LDH nanohybrid, the intensity of the (003) reflection peak gradually decreases and slightly shifts to the lower 2θ values, leading to a disordered structure, when compared to that of neat ZnAl-LDH. This may be due to fact that, the anions of HR quickly adsorb on the surface of the positively charged hydroxide layers once they are formed and become a platform for generating the next layer. Whilst the existence of the tiny anionic species (*i.e.* Cl^-, NO_3^- *etc.*) inhibits the intercalation of the relatively large and hydrophobic HR anions onto the hydrophilic hydroxide layers, it is expected to lead to a loose and disordered layer structure owing to incompatibility and steric hindrance.[57] Similar broad and low intensity XRD reflections derived from disordered layer stacking of MgAl-LDH during intercalation of hydrophobic drug prednisone is reported by Li *et al.*[58]

The intercalation of HR into the interlayers of the ZnAl-LDH host was investigated using FTIR spectroscopy. The FTIR spectra of neat HR, neat ZnAl-LDH, and LDH–HR are illustrated in Fig. 4. In the FTIR spectrum of ZnAl-LDH, the asymmetric stretching vibration of the interlayer LDH nitrate anions and the band characteristic of the hydroxyl group of the LDH layers are observed at 1378 and 3427 cm^{-1}, respectively, while the absorption peak at 1634 cm^{-1} is due to the bending vibration of water molecules.[57] The lattice vibration modes for M–O were detected at 607 cm^{-1}.[55] However, in the case of the neat HR, the spectrum shows many absorption bands and broad stretching vibrations for the resorcinol –OH groups are observed at 3422 and 3428 cm^{-1}, respectively. Furthermore, the FTIR peak at 2924 cm^{-1} is related to CH_2 asymmetric stretching vibration of the hexyl group. The bands between 1524 and 1452 cm^{-1} can be correlated to the stretching vibrations of the C=C bond in the benzene ring. The –OH bending vibration for the resorcinol –OH group is noted at 971 cm^{-1}. In the case of the LDH–HR nanohybrid, the spectrum has both the characteristic bands of neat HR and neat LDH along with slight shifts in position of some peaks (1524 to 1550 cm^{-1}, 1452 to 1457 cm^{-1}, 1378 to 1374 cm^{-1}, *etc.*), which indicates that the HR anions have been intercalated into the interlayer of the LDH host. Moreover, because of the intercalation of HR into LDH, the resorcinol –OH groups (3428 and 3422 cm^{-1}), and the bending vibration of the hydroxyl group (779 cm^{-1}) of the HR disappear while new phenoxide ion (PhO^-) bands appear at 920 and 1044 cm^{-1}. The broad absorption peak at 3412 cm^{-1} can be attributed to the presence of hydroxyl groups in the layers and the physically adsorbed water molecules.[55] The characteristic absorption bands at 1550, 1502, and 1457 cm^{-1} are assigned to the C=C stretching vibration of the benzene rings in LDH–HR, and the less intense peak at 1374 cm^{-1} was owing to the NO_3^- anion, which may not be completely removed from the interlayers during the intercalation, and due to the symmetric stretching vibration of the functional group.[59] Wang *et al.*[60] also observed similar weak vibration at 1386 cm^{-1} due to the co-existence of NO_3^- ion and antifolate drug methotrexatum intercalated in ZnAl-LDH prepared by co-precipitation.

The structure and morphology of the neat LDH and LDH–HR nanohybrid were studied using SEM and TEM microscopes. The SEM and TEM micrographs of neat LDH and the HR-intercalated LDH nanohybrid are shown in Fig. 5a, a1, b and b1. As shown in Fig. 5a and b, small platelets, along with irregular large thin flakes, with the mean diameters 5.4 ± 3.2 nm (Fig. 5c) are observed for ZnAl-LDH. The SEM image of the nanohybrid (Fig. 5a1) shows bigger polygonal plate-like morphology, which suggests aggregation of LDH particles in presence of HR. Furthermore, distinct platelets of different sizes are clearly visible in the TEM micrograph of LDH (Fig. 5b)

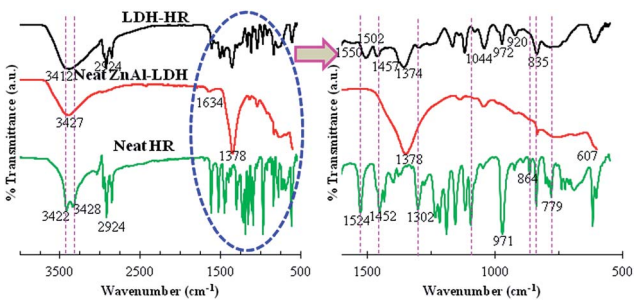

Fig. 4 FTIR spectra of neat HR, ZnAl-LDH, and LDH–HR.

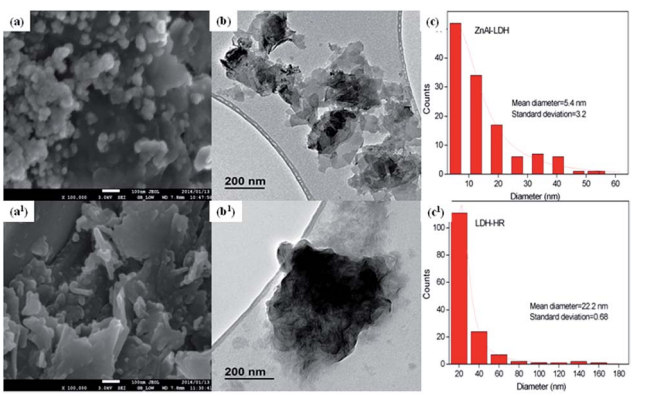

Fig. 5 FE-SEM (a and a[1]), TEM (b and b[1]) images and particle size distribution (c and c[1]) of ZnAl-LDH and LDH–HR nanohybrid prepared by co-precipitation method.

whereas, LDH–HR nanohybrid shows some bigger and aggregated structure (Fig. 5b1), which could also be correlated with the loss of crystallinity due to the intercalation of HR. Intercalation of HR molecules into LDH host layers increases the mean particle diameter from 5.4 nm to 22.2 nm (Fig. 5c and c1), which also indicates possible aggregation during intercalation. These results are in line with the XRD patterns and have close similarity to the change of discrete plate-like morphology to agglomerated non-porous granular structure of MgAl-LDH after intercalation of hydrophobic anticancer drug, raloxifene hydrochloride as recently reported by Senapati and co-workers.[61]

The particle sizes obtained from dynamic light scattering follows the same trend as observed in TEM results (Table 2). The mean particle size increases from 0.29 to 0.51 μm after the incorporation of HR due to aggregation of particles. Both samples show a broad particle size distribution as indicated by the polydispersity index above 20%.[62] The zeta-potential of +24.9 in the case of ZnAl-LDH is attributed to the surface positive charge[63] while the value of −16.2 in LDH–HR suggests the presence of negatively charged active molecules on the surface. The absolute value of zeta potential for LDH–HR is below 25 mV which shows that the particles will not be stable in aqueous dispersions.[64] Hence, LDH–HR is added to the oil phase prior to mixing and formulation is further stabilized by emulsifiers.

TGA and differential thermal analysis curves of neat HR, neat ZnAl-LDH, and the LDH–HR nanohybrid are illustrated in Fig. 6. The TGA/DTA curves for HR show a single weight loss stage and a sharp, intense peak at 218 °C corresponding to 80.1% weight loss, which was due to the combustion of HR. The thermal decomposition of neat ZnAl-LDH shows that the mass loss occurs in four major steps at 104.5 °C, 208.2 °C, 270.4 °C and 608.1 °C, with corresponding weight losses of 6.9%, 16.1%, 23.6%, and 38.2%, respectively. The first step of weight loss in the range of 73–144 °C is associated with the removal of the water molecules physically adsorbed on the surfaces layers.[54] The second and third weight losses in the ranges of 145–239 °C and 243–298 °C are due to the dehydroxylation of the metal hydroxide layers and the decomposition of nitrate anions, respectively. The final step of weight loss at 516–645 °C is associated with the decomposition of residual adsorbed nitrate and the collapse along with the dehydroxylation of the layers of ZnAl-LDH and the formation of metal oxides.[65] The LDH–HR nanohybrid also exhibits four major thermal decomposition temperatures at 80.4 °C, 146.5 °C, 205.5 °C and 330.4 °C, with weight losses of 7.8%, 17.4%, 35.7% and 55.3%, respectively. The 7.8% weight loss, which occurred at 80 °C, is ascribed to the removal of physically absorbed water. The weight loss increases

Table 2 Particle size and zeta potential of ZnAl-DH and LDH–HR

Samples	Hydrodynamic diameter (μm)	Polydispersity index (%)	Mean zeta potential (mV)
ZnAl-LDH	0.296	38.8	+24.9 ± 1.3
LDH–HR	0.513	35.4	−16.2 ± 0.5

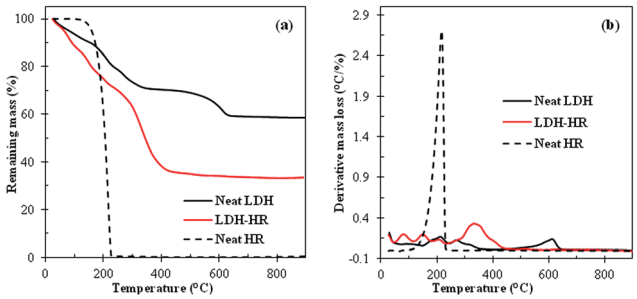

Fig. 6 TG and DTA curves of neat LDH, HR, and the LDH–HR nanohybrids.

to 55.3% at 330.4 °C due to the decomposition of HR anions, dehydroxylation of inorganic layers, and formation of Zn and Al oxides. The increase in the decomposition temperature of HR from 218.2 °C (for neat HR) to 330.4 °C (for the nanohybrid) indicates increased thermal stability of HR in the intercalated hybrid in comparison to that of free HR molecules, which is owing to the electrostatic interaction (attraction) and/or formation of the hydrogen bonds between the positively charged brucite-like layers of ZnAl-LDH and the negatively charged functional group of HR. The residue left after combustion of unmodified LDH at 900 °C is 58.4% while 33.37% residue is found at same temperature for LDH–HR nanohybrid. Considering the formation of metal oxides at high temperature, the difference in residue obtained is proportional to active ingredient loading capacity of LDH host layer which is calculated to be 25.1% under the used synthesis conditions. Deyi *et al.*[66] also used TGA residue analysis to calculate the extent of organic modification of CoAl-LDH by dodecyl benzene sulphonate.

In vitro release studies of HR from the LDH–HR nanohybrid

The release behaviour of HR anions from the ZnAl-LDH host in PBS medium obtained from UV-Vis analyses is shown in Fig. 7.

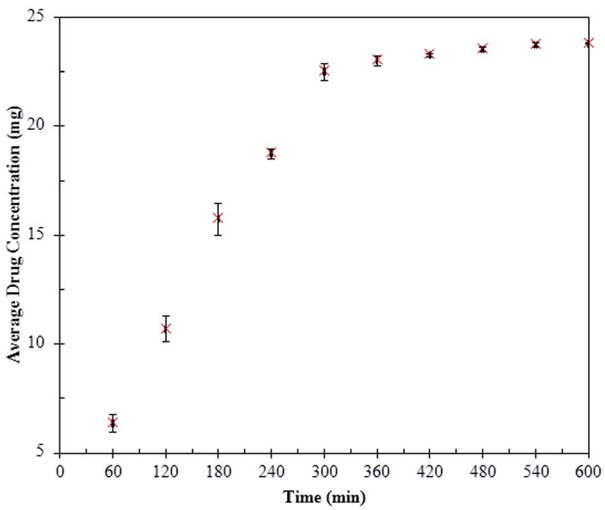

Fig. 7 Release profile of HR anion from the LDH host in PBS solution.

The LDH–HR nanohybrid in PBS (pH 7.4) shows a gradual release pattern upto 300 min, releasing 48.7% HR followed by a relatively slow release (88.6% in 540 min), eventually reaching a steady state. The long-standing release performance play a significant role in therapeutic treatments, as the early fast release rapidly allows a therapeutic dosage and the following sustained release continues this dose over a long period of time.[51,67] Considering the fact that the nanohybrid is synthesized at alkaline pH, the initial rapid release can be attributed to the dissolution of LDH in a lower pH PBS medium and subsequent diffusion of HR molecules. This can also happen if some of the HR molecules are adsorbed on the LDH surface rather than intercalated into the interlayer space. During the release process, the HR that leaves the LDH interlayer region is being continuously replaced by phosphate ions ($H_3PO_4^-$) from the PBS solution. Initially, the concentration of HR in the inner layer region of LDH is high, causing the faster release. Consequently, the release of HR slows down over time as it emigrates from the host and new LDH barrier with counter ion is formed, thus suggesting that concentration of HR and affinity of exchangeable anion in the medium are contributing factors to the rate of active ingredient release.[51,68] It is also noteworthy that intercalation of HR to LDH layers also inhibits complete release of HR even after 600 min which suggest that ZnAl-LDH are suitable materials as controlled release host. The release pattern of HR from LDH is similar to release of other pharmaceutical drugs from LDH layers described in the literature.[51,69]

In vivo studies of the LDH–HR nanohybrid-based topical application

The blotch test for a cosmetic product is used to check the compatibility of a formulation with the human skin before its application. The O/W emulsion topical composition including the nanohybrid was ideally applied for at least twice per day for two weeks, and no skin irritation was observed after the application on the forearms of the healthy human volunteers. Therefore, the developed formulation with the nanohybrid was considered well suited and reasonably safe for human use.

In the course of the *in vivo* study for 3 weeks, significant changes in melanin contents were observed in both the neat HR and the LDH–HR formulations. The LDH–HR cream significantly minimizes the melanin content of the skin after 2 weeks. The data collected are presented as mean ± standard deviation on four volunteers (V1–V4) in Table 3. As seen in table, the base line (untreated) melanin content shows different values; 68 ± 2.54 for V1, 76 ± 3.54 for V2, 76 ± 4.34 for V3, and 60 ± 0.98 for V4, respectively, which corresponds to varying skin tones of different volunteers. On regular application of the formulation, the melanin contents decreases significantly after one week and further reduction is observed during second and third week. Our data clearly show that, the inclusion of LDH–HR nanohybrid in the formulation reduced melanin content from 68 ± 2.54 to 61.5 ± 3.40 for V1, 76 ± 3.54 to 57.6 ± 5.21 for V2, 76 ± 4.34 to 65.3 ± 4.95 for V3, and 60 ± 0.98 to 52.6 ± 2.86 for V4, respectively. This indicates that the inorganic LDH is a contributing factor in the faster skin absorption/adhesion and release of HR molecules, which leads to more noticeable results than those observed for neat HR.

The LDH–HR nanohybrid can act as inorganic solid particles that stabilize the emulsion (Pickering emulsions). Several groups reported accelerated transport of drug from emulsions containing solid particles in comparison to the conventional surfactant only emulsions. Higher accumulation and bioavailability of hydrophobic all *trans*-retinol and hydrophilic caffeine in dermis through application of Pickering emulsions containing silica nanoparticles have been reported by Frelichowska *et al.*[70] and Eskandar *et al.*[71] According to them, the higher adhesion energy for drops of Pickering emulsion gives longer contact time for the effective transfer of active molecules to the skin and this compensates for the penetration enhancing activity of surfactant in conventional emulsion through fluidization of intracellular matrix of *stratum corneum*. It is well demonstrated that the inorganic particles do not penetrate deeply and their availability is restricted to the *stratum corneum*.[72]

Applying similar model, it can be explained that the LDH–HR nanohybrid in the formulation is better absorbed and adhered to the skin due to the hydrophobic nature of LDH after intercalation. The HR molecules from the nanohybrid are released in a controlled manner through ion exchange with the anionic species present in skin wastes, sera, and sweat. The active ingredient released can then travel deeper through the

Table 3 Results of the statistical analysis of melanin content and erythema score for four volunteers after topical application of neat HR and LDH–HR based formulation

		Time interval							
		Neat HR				LDH–HR nanohybrid			
		Baseline	D7	D14	D21	Baseline	D7	D14	D21
V1	Melanin	65 ± 0.84	61.4 ± 3.13	59.66 ± 2.74	59.16 ± 2.73	68 ± 2.54	65.8 ± 2.31	63.16 ± 3.23	61.5 ± 3.40
	Erythema	61.05 ± 1.08	58 ± 3.4	57.83 ± 2.19	57.83 ± 2.67	69 ± 1.62	59 ± 3.68	58.16 ± 3.18	58.5 ± 4.89
V2	Melanin	68.02 ± 1.54	68.4 ± 1.01	66.83 ± 1.34	67 ± 0.81	76 ± 3.54	61.6 ± 3.92	59.5 ± 4.34	57.6 ± 5.21
	Erythema	62.1 ± 1.62	64 ± 2.28	67.66 ± 3.59	63.16 ± 3.43	73 ± 0.85	58 ± 4.6	60.5 ± 2.98	61.16 ± 3.71
V3	Melanin	71.24 ± 2.04	68.2 ± 2.31	64.5 ± 3.09	64.66 ± 2.92	76 ± 4.34	70 ± 4.4	64.5 ± 5.43	65.3 ± 4.95
	Erythema	57 ± 2.61	58.2 ± 3.76	57.83 ± 2.26	59 ± 2.58	67 ± 2.12	59.6 ± 4.27	58.8 ± 5.17	58.3 ± 3.98
V4	Melanin	55.54 ± 1.32	52.8 ± 1.93	52.33 ± 1.49	52.5 ± 1.25	60 ± 0.98	55 ± 2.28	54 ± 2.30	52.6 ± 2.86
	Erythema	54.37 ± 0.78	56.6 ± 2.57	55 ± 1.63	55.16 ± 1.77	63 ± 1.57	56.6 ± 1.01	56.1 ± 1.57	56.3 ± 1.69

skin layers to the site of action, thus enhancing its bioavailability and tyrosinase and melanogenesis inhibition activity.[73]

The comparison of the statistical data obtained for erythema score for four volunteers are also shown in Table 3. It is noteworthy that, while the LDH–HR formulation decreases the erythema level uniformly on the applied skin area over the period of 3 weeks, irregular effects of the application of the neat HR formulation on erythema level are observed. Significant reduction in erythema score indicates that the formulation containing LDH–HR is unlikely to cause any skin irritation. Therefore, it is evident that the LDH act as an effective carrier and delivery system for HR molecules.

Based on these results, we conclude that the inorganic LDHs can act as efficient controlled delivery vehicle for active ingredients in topical applications and such delivery systems in the cosmetic industry in the future and can overcome the problems associated with direct addition of active molecules in formulations and their skin compatibility.

4 Conclusion

In this study, we developed a new class of nanohybrids and evaluated their inhibitory effects on tyrosinase activity and melanogenesis. Our data verified the efficiency of the LDH–HR nanohybrid in modulating skin pigmentation. It was also confirmed that the even skin tone effect was produced by inhibition of the activity of tyrosinase enzyme and the inhibition on melanogenesis. These results indicated LDH–HR nanohybrid to be a safe and effective agent that can be used for correcting uneven human skin tone in 14 days.

Acknowledgements

DM sincerely acknowledges the Directors of Amka Products Pty Ltd, South Africa, for their financial and laboratory facilities. The author also wishes to especially thank Mr Nazir Kalla, Mr Hussain Kalla, Prof. Victor Witlock, Dr Manfred Scriba, and Dr James Wesley Smith. The authors LM, SP, and SSR are further thankful to the Department of Science and Technology (HGERA8X) and the Council for Scientific and Industrial Research (HGER20S) for providing their laboratory and characterization facilities and financial support.

References

1 V. Rives, M. del Arco and C. Martín, *J. Controlled Release*, 2013, **169**, 28–39.
2 B. Peter, D. P. Pioletti, S. Laïb, B. Bujoli, P. Pilet, P. Janvier, J. Guicheux, P. Y. Zambelli, J. M. Bouler and O. Gauthier, *Bone*, 2005, **36**, 52–60.
3 S. Zhang, Z. Chu, C. Yin, C. Zhang, G. Lin and Q. Li, *J. Am. Chem. Soc.*, 2013, **135**, 5709–5716.
4 H. Zhang, D. Pan, K. Zou, J. He and X. Duan, *J. Mater. Chem.*, 2009, **19**, 3069–3077.
5 Y. Cheng, A. C. Samia, J. D. Meyers, I. Panagopoulos, B. Fei and C. Burda, *J. Am. Chem. Soc.*, 2008, **130**, 10643–10647.
6 P. a. Ma, H. Xiao, C. Li, Y. Dai, Z. Cheng, Z. Hou and J. Lin, *Mater. Today*, 2015, **18**, 554–564.
7 Z. Liu, K. Chen, C. Davis, S. Sherlock, Q. Cao, X. Chen and H. Dai, *Cancer Res.*, 2008, **68**, 6652–6660.
8 V. R. R. Cunha, V. A. Guilherme, E. de Paula, D. R. de Araujo, R. O. Silva, J. V. R. Medeiros, J. R. S. A. Leite, P. A. D. Petersen, M. Foldvari, H. M. Petrilli and V. R. L. Constantino, *Mater. Sci. Eng., C*, 2016, **58**, 629–638.
9 Q. Wang and D. O'Hare, *Chem. Rev.*, 2012, **112**, 4124–4155.
10 H. Nakayama, N. Wada and M. Tsuhako, *Int. J. Pharm.*, 2004, **269**, 469–478.
11 S. Aisawa, H. Kudo, T. Hoshi, S. Takahashi, H. Hirahara, Y. Umetsu and E. Narita, *J. Solid State Chem.*, 2004, **177**, 3987–3994.
12 S. Mallakpour and M. Dinari, *J. Therm. Anal. Calorim.*, 2015, **119**, 1123–1130.
13 M. S. Gasser, *Colloids Surf., B*, 2009, **73**, 103–109.
14 X. Gao, L. Lei, D. O'Hare, J. Xie, P. Gao and T. Chang, *J. Solid State Chem.*, 2013, **203**, 174–180.
15 J. Meng, H. Zhang, D. G. Evans and X. Duan, *Chin. Sci. Bull.*, 2005, **50**, 745–751.
16 I. Pavlovic, M. A. González, F. Rodríguez-Rivas, M. A. Ulibarri and C. Barriga, *Appl. Clay Sci.*, 2013, **80–81**, 76–84.
17 M. Wei, M. Pu, J. Guo, J. Han, F. Li, J. He, D. G. Evans and X. Duan, *Chem. Mater.*, 2008, **20**, 5169–5180.
18 P. Gunawan and R. Xu, *Chem. Mater.*, 2009, **21**, 781–783.
19 F. Li, L. Jin, J. Han, M. Wei and C. Li, *Ind. Eng. Chem. Res.*, 2009, **48**, 5590–5597.
20 M.-A. Thyveetil, P. V. Coveney, H. C. Greenwell and J. L. Suter, *J. Am. Chem. Soc.*, 2008, **130**, 12485–12495.
21 M.-A. Thyveetil, P. V. Coveney, H. C. Greenwell and J. L. Suter, *J. Am. Chem. Soc.*, 2008, **130**, 4742–4756.
22 K. Ladewig, M. Niebert, Z. P. Xu, P. P. Gray and G. Q. M. Lu, *Biomaterials*, 2010, **31**, 1821–1829.
23 A. C. S. Alcantara, P. Aranda, M. Darder and E. Ruiz-Hitzky, *J. Mater. Chem.*, 2010, **20**, 9495–9504.
24 Z. Gu, A. C. Thomas, Z. P. Xu, J. H. Campbell and G. Q. Lu, *Chem. Mater.*, 2008, **20**, 3715–3722.
25 L. Jin, Q. Liu, Z. Sun, X. Ni and M. Wei, *Ind. Eng. Chem. Res.*, 2010, **49**, 11176–11181.
26 Q. Zheng, Y. Hao, P. Ye, L. Guo, H. Wu, Q. Guo, J. Jiang, F. Fu and G. Chen, *J. Mater. Chem. B*, 2013, **1**, 1644–1648.
27 S. H. Hussein Al Ali, M. Al-Qubaisi, M. Z. Hussein, M. Ismail, Z. Zainal and M. N. Hakim, *Int. J. Nanomed.*, 2012, **7**, 2129–2141.
28 M. Badar, M. I. Rahim, M. Kieke, T. Ebel, M. Rohde, H. Hauser, P. Behrens and P. P. Mueller, *J. Biomed. Mater. Res., Part A*, 2015, **103**, 2141–2149.
29 B. Li, J. He, D. G. Evans and X. Duan, *Int. J. Pharm.*, 2004, **287**, 89–95.
30 L. Qin, M. Xue, W. Wang, R. Zhu, S. Wang, J. Sun, R. Zhang and X. Sun, *Int. J. Pharm.*, 2010, **388**, 223–230.
31 S. Briganti, E. Camera and M. Picardo, *Pigm. Cell Res.*, 2003, **16**, 101–110.
32 F. Solano, S. Briganti, M. Picardo and G. Ghanem, *Pigm. Cell Res.*, 2006, **19**, 550–571.

33 Y.-K. Won, C.-J. Loy, M. Randhawa and M. D. Southall, *Arch. Dermatol. Res.*, 2014, **306**, 455–465.
34 B. Kasraee, F. Handjani, A. Parhizgar, G. R. Omrani, M. R. Fallahi, M. Amini, M. Nikbakhsh, C. Tran, A. Hügin, O. Sorg and J. H. Saurat, *Dermatology*, 2005, **211**, 360–362.
35 J. L. Sanchez and M. Vazquez, *Int. J. Dermatol.*, 1982, **21**, 55–59.
36 H. Shimogaki, Y. Tanaka, H. Tamai and M. Masuda, *Int. J. Cosmet. Sci.*, 2000, **22**, 291–303.
37 W. H. Kang, S. C. Chun and S. Lee, *J. Dermatol.*, 1998, **25**, 587–596.
38 L. S. Kakita and N. J. Lowe, *Clin. Ther.*, 1998, **20**, 960–970.
39 A. L. Haddad, L. F. Matos, F. Brunstein, L. M. Ferreira, A. Silva and D. Costa, *Int. J. Dermatol.*, 2003, **42**, 153–156.
40 A. P. DeCaprio, *Crit. Rev. Toxicol.*, 1999, **29**, 283–330.
41 G. H. Findlay, J. G. L. Morrison and I. W. Simson, *Br. J. Dermatol.*, 1975, **93**, 613–622.
42 R. A. Hoshaw, K. G. Zimmerman and A. Menter, *Arch. Dermatol.*, 1985, **121**, 105–108.
43 J. H. Kraal, A. A. Hussain, S. B. Gregorio and E. Akaho, *J. Dent. Res.*, 1979, **58**, 2125–2131.
44 V. H. Frankos, D. F. Schmitt, L. C. Haws, A. J. McEvily, R. Iyengar, S. A. Miller, I. C. Munro, F. M. Clydesdale, A. L. Forbes and R. M. Sauer, *Regul. Toxicol. Pharmacol.*, 1991, **14**, 202–212.
45 J. G. Buta, H. E. Moline, D. W. Spaulding and C. Y. Wang, *J. Agric. Food Chem.*, 1999, **47**, 1–6.
46 G. C. Yen, P. D. Duh and C. W. Lin, *Free Radical Res.*, 2003, **37**, 509–514.
47 D. McNally, A. Shephard and E. Field, *J. Pharm. Pharm. Sci.*, 2012, **15**, 281–294.
48 Q. X. Chen, L. N. Ke, K. K. Song, H. Huang and X. D. Liu, *Protein J.*, 2004, **23**, 135–141.
49 L. Kolbe, T. Mann, W. Gerwat, J. Batzer, S. Ahlheit, C. Scherner, H. Wenck and F. Stäb, *J. Eur. Acad. Dermatol. Venereol.*, 2013, **27**, 19–23.
50 Y. K. Won, C. J. Loy, M. Randhawa and M. D. Southall, *Arch. Dermatol. Res.*, 2014, **306**, 455–465, references there in.
51 Z. Meng, X. Li, F. Lv, Q. Zhang, P. K. Chu and Y. Zhang, *Colloids Surf., B*, 2015, **135**, 339–345.
52 Y. Zhang and J. R. G. Evans, *Colloids Surf., A*, 2012, **408**, 71–78.
53 J. Olanrewaju, B. L. Newalkar, C. Mancino and S. Komarneni, *Mater. Lett.*, 2000, **45**, 307–310.
54 L. Li, R. Ma, Y. Ebina, N. Iyi and T. Sasaki, *Chem. Mater.*, 2005, **17**, 4386–4391.
55 F. Barahuie, M. Z. Hussein, S. A. Gani, S. Fakurazi and Z. Zainal, *J. Solid State Chem.*, 2015, **221**, 21–31.
56 V. J. Nagaraj, X. Sun, J. Mehta, M. Martin, T. Ngo and S. K. Dey, *J. Nanotechnol.*, 2015, **2015**, 10.
57 M. Zobir bin Hussein, A. Hj Yahaya, Z. Zainal and L. Hee Kian, *Sci. Technol. Adv. Mater.*, 2005, **6**, 956–962.
58 Y. Li, H. Li, M. Wei, J. Lu and L. Jin, *Chem. Eng. J.*, 2009, **151**, 359–366.
59 S. H. Hussein Al Ali, M. Al-Qubaisi, M. Z. Hussein, M. Ismail, Z. Zainal and M. N. Hakim, *Int. J. Nanomed.*, 2012, **7**, 4251–4262.
60 W. Wang, H. Liu, S. Li and X. Li, *Appl. Clay Sci.*, 2016, **121–122**, 103–110.
61 S. Senapati, R. Thakur, S. P. Verma, S. Duggal, D. P. Mishra, P. Das, T. Shripathi, M. Kumar, D. Rana and P. Maiti, *J. Controlled Release*, 2016, **224**, 186–198.
62 S. Khurshid, E. Saridakis, L. Govada and N. E. Chayen, *Nat. Protoc.*, 2014, **9**, 1621–1633.
63 Z. P. Xu, Y. Jin, S. Liu, Z. P. Hao and G. Q. Lu, *J. Colloid Interface Sci.*, 2008, **326**, 522–529.
64 F. H. Bijarbooneh, Y. Zhao, J. H. Kim, Z. Sun, V. Malgras, S. H. Aboutalebi, Y. Heo, M. Ikegami and S. X. Dou, *J. Am. Ceram. Soc.*, 2013, **96**, 2636–2643.
65 S. M. N. Mohsin, M. Z. Hussein, S. H. Sarijo, S. Fakurazi, P. Arulselvan and T.-Y. Y. Hin, *Chem. Cent. J.*, 2013, **7**, 26.
66 W. De-yi, A. Leuteritz, U. Wagenknecht and G. Heinrich, *Trans. Nonferrous Met. Soc. China*, 2009, **19**, 1479–1482.
67 X. Kong, L. Jin, M. Wei and X. Duan, *Appl. Clay Sci.*, 2010, **49**, 324–329.
68 S. H. Sarijo, M. Z. Hussein, A. H. J. Yahaya and Z. Zainal, *J. Hazard. Mater.*, 2010, **182**, 563–569.
69 X. Bi, H. Zhang and L. Dou, *Pharmaceutics*, 2014, **6**, 298–332.
70 J. Frelichowska, M.-A. Bolzinger, J.-P. Valour, H. Mouaziz, J. Pelletier and Y. Chevalier, *Int. J. Pharm.*, 2009, **368**, 7–15.
71 G. Eskandar, S. Simovic and C. A. Prestidge, *Pharm. Res.*, 2009, **26**, 1764–1775.
72 M.-A. Bolzinger, S. Briançon and Y. Chevalier, *Wiley Interdiscip. Rev.: Nanomed. Nanobiotechnol.*, 2011, **3**, 463–478.
73 M. Schneider, F. Stracke, S. Hansen and U. F. Schaefer, *Derm.-Endocrinol.*, 2009, **1**, 197–206.